Classical and thermodynamic limits in a system of interacting quantum spins

1996 J. Phys. A: Math. Gen. 29 3143

(http://iopscience.iop.org/0305-4470/29/12/020)

J. Phys. A: Math. Gen. **29** (1996) 3143–3166. Printed in the UK

Classical and thermodynamic limits in a system of interacting quantum spins

Allan K Evans†

Cavendish Laboratory, Cambridge CB3 0HE, UK

Received 12 September 1995

Abstract. We study a model system composed of interacting quantum spins, with every spin coupled to every other, in the limit where the number of spins K and the angular momentum j of each spin are both large, aiming to explore the effect of large system size on the breakdown of the classical limit of quantum mechanics. We obtain the exact spectrum of the Hamiltonian, and hence the trace $\mathcal{U}(\tau)$ of the quantum-mechanical time-evolution operator. We examine the time dependence of $\mathcal{U}(\tau)$, finding a simple approximation which is valid when j and K are large. At a time proportional to $j\sqrt{K}$, this approximation breaks down, and the long-time behaviour is extremely complex. We use a renormalization scheme to investigate this complexity. The scheme is based upon a generalization of the Gauss continued-fraction map to the complex plane.

1. Introduction

Both the classical and the thermodynamic limits are important to our understanding of the world in terms of fundamental physical laws. We can regard most everyday objects as practically infinite on an atomic scale, and this justifies the use of the thermodynamic limit, where the size of a system is taken to be infinite. Similarly, the Planck constant is so small that quantum effects are completely negligible in everyday life. This is the reason that the existence of quantum mechanics was not suspected until the twentieth century.

Since these limiting cases of the fundamental laws are so commonly used and so important to physics, it is unfortunate that the limits involved are not simple or mathematically well behaved. Berry [1] has discussed this problem in general. In this paper, we investigate a simple quantum system where both the classical and the thermodynamic limits can be explored, hoping to shed some light upon the combined effect of the two limits. Our main conclusion will be that at long times, the classical and thermodynamic limits lead to extremely complex behaviour. This is in contrast to the simplicity of the time dependence at short times in these limits.

Since in both classical and thermodynamic limits, the quantum density of states becomes large, we might expect to find analogies between the two limits. For example, it is well known that approximations which are valid for large quantum numbers, and also those which are valid for large system size, often break down at long times.

In the field of research known as 'quantum chaology', this observation resolves a paradox. Consider the quantum-mechanical version of a chaotic classical dynamical system. Since a finite quantum system has a purely discrete spectrum, its time dependence must be

† Now at: Department of Mathematical Sciences, De Montfort University, Leicester LE1 9BH, UK.

0305-4470/96/123143+24$19.50

quasiperiodic, and therefore not chaotic. But the Ehrenfest correspondence theorem claims that in the classical limit, the quantum mechanics of the system must approach the chaotic classical behaviour.

This apparent paradox is resolved by the observation that there are two time-scales involved. For short times, quantum-mechanical wavepackets follow classical trajectories, which may be chaotic. However, over large time-scales, the classical limit breaks down, the quantum-mechanical nature of the system becomes apparent and the motion is quasiperiodic. This subject was reviewed by Chirikov *et al* [2]. More recently, detailed studies [3] of the quantum time evolution of classically chaotic systems have suggested that, in general, the semiclassical approximation breaks down at some critical time

$$\tau_{\bar{h}} \sim \frac{1}{\lambda} \log\left(\frac{I}{\bar{h}}\right) \tag{1}$$

where λ is the largest Lyapounov exponent and I is proportional to the size of the phase space. A simple argument for this result is as follows [3]. A wavepacket representing a quantum particle cannot be localized on a scale smaller than $\bar{h}$ (or perhaps $\bar{h}^{1/2}$—this makes no difference to the argument), because of the uncertainty principle. For a chaotic system, trajectories diverge exponentially with time as $e^{\lambda t}$. Hence after time t, the extent of a wavepacket is of the order of $\bar{h}\, e^{\lambda t}$. The semiclassical approximation breaks down when the wavepacket has spread out so that its size is of the order of the size I of the phase space. Hence we have a critical time as in equation (1).

For non-chaotic systems, this argument must be modified because trajectories diverge with time, not exponentially, but linearly. In this case we would expect a time-scale

$$\tau_{\bar{h}} \sim \frac{I}{\bar{h}}\,. \tag{2}$$

The results which we shall derive for our simple model system will be closer to equation (2) than to equation (1), suggesting that the classical version of the system is not chaotic.

In non-equilibrium statistical mechanics, the thermodynamic limit is often invoked to derive irreversible behaviour such as the approach to equilibrium. The approximations used here also break down at long times. Two examples are the harmonic-oscillator assembly of Mazur and Montroll [4], and the rigorous derivation of the Boltzmann equation for a hard-sphere gas, first given by Lanford [5], and discussed by Spohn [6].

In this paper, we investigate a model system composed of quantum spins. We calculate the trace of the quantum-mechanical evolution operator for large values of the number of spins K and the magnitude of each spin j. The trace is a typical time-dependent quantity because it contains the time dependences of all the energy eigenstates of the system. We find that a simple approximation is valid in the limit where both j and K are large, but that this approximation breaks down at large times, just as we would expect a semiclassical approximation to break down. The time at which the approximation ceases to be valid is proportional to $j\sqrt{K}$. For times longer than this, the time dependence is extremely complicated.

In the next section, we briefly review some earlier work on the properties of classical and thermodynamic limits in quantum spin systems. In sections 3–5, we introduce the spin system which is the subject of the present paper, obtain the spectrum of the Hamiltonian, and find the trace of the evolution operator. A simple approximation for the time dependence of the trace at short times is derived.

In section 6, we study the long-time behaviour of the trace. We use a renormalization scheme which depends upon some properties of elliptic functions and a generalization of Gauss's continued-fraction mapping. A related scheme was used by Berry and Goldberg

[7] to study a single precessing quantum spin. We find that the long-time behaviour of the trace is complex, with complexity growing as we increase j and K.

2. Previous work on quantum spin systems

Theoretical work on quantum-mechanical spin systems has been concentrated in two areas: the thermodynamic limit where the number of spins is large, and the classical limit where the magnitude of each spin is large. A review of the nature of integrability in both cases has been given by Müller [8].

Fisher [9] was the first to consider the classical limit of a quantum-mechanical spin chain. He derived the partition function for a linear Heisenberg model with isotropic nearest-neighbour coupling in the classical case, and compared the thermodynamics of the model with that of quantum spin chains. Millard and Leff [10] put this work on a rigorous base with a proof that for a Heisenberg model with any coupling, the classical limit of the quantum canonical partition function is the classical partition function.

More recently, the study of 'quantum chaos' has revived interest in the classical limit, and a number of studies of small clusters of quantum spins in the classical limit have been made [11–13]. These studies have mostly focused on the distribution of eigenvalues of the Hamiltonian. However, Berry and Goldberg [7] have found surprisingly complex time dependence in the trace of the evolution operator for a single precessing spin.

Exactly-solved models of large quantum systems have generally been restricted to the case of spin-$\frac{1}{2}$ particles. Examples are the isotropic linear Heisenberg model, which was solved by Bethe [14] with his ansatz, and the XY model of Lieb *et al* [15]. Neither the Bethe ansatz nor the transformation to a representation in terms of fermion operators which is used for the XY model generalizes to spins of magnitude greater than $\frac{1}{2}$. Reprints of these papers and many others are included in a fascinating collection compiled by Mattis [16].

We should also mention the work of Berman and Zaslavsky on atoms interacting with a radiation field [3]. Both integrable and non-integrable (chaotic) versions of this system were considered. Numerical studies showed that the dependence of the time-scale $\tau_{\bar{h}}$ on $\bar{h}$ was logarithmic, as in equation (1) in the non-integrable case, and linear, as in equation (2), when the system was integrable.

As far as the author knows, no analytical results have been published on the properties of large systems in the classical limit. The present work is intended as a beginning to the study of this problem, which has obvious physical importance.

3. The model

The model system which is the subject of this paper consists of K quantum spins, each with angular momentum quantum number j, interacting via the Hamiltonian

$$H = -\bar{\gamma} \sum_{i,j} \boldsymbol{s}_i \cdot \boldsymbol{s}_j. \tag{3}$$

We can picture this Hamiltonian as representing a cluster of spins, each spin interacting equally with every other spin in the cluster. A less physical interpretation is to think of the spins as being placed on a network which is a complete graph; that is, where every site is connected to every other site.

The equilibrium statistical mechanics of physical systems placed on a complete graph has been the subject of some interest. A model proposed by Tóth [17], and investigated

first by Tóth and then by Penrose [18], consisting of a lattice gas of bosons with hard-core repulsions, was the first interacting system where Bose condensation was demonstrated to occur.

The model Hamiltonian (3) arises when we apply the mean-field approximation to a Heisenberg model of interacting spins with some local interaction J_{ij}. The Heisenberg Hamiltonian is

$$H_{\mathrm{H}} = -\sum_{i \neq j} J_{ij} \boldsymbol{s}_i \cdot \boldsymbol{s}_j \,. \tag{4}$$

In the mean-field approximation, we replace one of the spin operators $\boldsymbol{s}_j$ in each product $\boldsymbol{s}_i \cdot \boldsymbol{s}_j$ with $\bar{\boldsymbol{s}}$, the average over the whole system:

$$\bar{\boldsymbol{s}} = \frac{1}{K} \sum_{l=1}^{K} \boldsymbol{s}_l \,. \tag{5}$$

Assuming that the interaction J_{ij} is translationally invariant, we then obtain the Hamiltonian

$$-\left(\frac{1}{K} \sum_{j} J_{ij} \right) \sum_{i,l} \boldsymbol{s}_i \cdot \boldsymbol{s}_j \tag{6}$$

which is just the model Hamiltonian (3), with

$$\bar{\gamma} = \frac{1}{K} \sum_{j} J_{ij} \,. \tag{7}$$

In the present paper, we shall be investigating the behaviour of this model in the limits where the number of spins, K, and the magnitude of each spin, j, become large. It is therefore important to decide upon the scaling behaviour of the interaction $\bar{\gamma}$ as we increase the parameters K and j. We take $\bar{\gamma}$ to be inversely proportional to the system size K, as in equation (7), so that the total energy scales linearly with K. As we take the semiclassical limit $j \to \infty$, we hold the spin–spin interaction energy, which is of order $j^2\bar{\gamma}$, constant. The interaction parameter $\bar{\gamma}$ will therefore be written as

$$\bar{\gamma} = \frac{\gamma}{Kj(j+1)} \tag{8}$$

where γ is a coupling constant independent of K and j.

4. The spectrum of the Hamiltonian

We shall not attempt to find the energy eigenstates of the Hamiltonian (3) in terms of the individual spin states. We consider only the eigenvalues E_J and their degeneracies. We shall derive approximate expressions for the degeneracies, which are valid in the limit where j and K are large. This information will be used to investigate the behaviour of the trace of the quantum time-evolution operator, in the combined limit $j, K \to \infty$.

4.1. Eigenvalues

We shall be able to find the eigenvalues of the model Hamiltonian (3) without difficulty because the Hamiltonian is closely related to the total angular momentum of the system. Since the total angular momentum operator is

$$\boldsymbol{J} = \sum_{i} \boldsymbol{s}_i \tag{9}$$

we have simply

$$H = -\bar{\gamma}\boldsymbol{J}^2 . \tag{10}$$

The eigenvalues of H are therefore

$$\begin{aligned} E_J &= -J(J+1)\bar{\gamma}\bar{h}^2 \\ &= -\frac{J(J+1)\gamma\bar{h}^2}{Kj(j+1)} . \end{aligned} \tag{11}$$

For simplicity, we assume that j is an integer, so that J also ranges over integer values. The range of J is

$$0 \leqslant J \leqslant Kj . \tag{12}$$

To determine the energy spectrum of H, we need only find the degeneracy N_J of each eigenvalue E_J.

4.2. Degeneracies

We define the total spin quantum numbers J and M by the eigenvalue equations

$$\boldsymbol{J}^2|J, M\rangle = \bar{h}^2 J(J+1)|J, M\rangle \tag{13}$$

and

$$J_z|J, M\rangle = \bar{h}M|J, M\rangle . \tag{14}$$

The components (J_x, J_y, J_z) of the operator $\boldsymbol{J}$ have all the well known [19] properties of angular momentum operators. In particular, by acting upon a quantum state $|J, M\rangle$ with the ladder operators

$$J_\pm = J_x \pm \mathrm{i}J_y \tag{15}$$

we can construct a family of $(2J+1)$ states, sharing the same J, but each having a different integer value of M in the range $-J \leqslant M \leqslant J$. This means that the degeneracy of the quantum number J must be a multiple of $(2J+1)$. We write

$$N_J = (2J+1)\bar{N}_J . \tag{16}$$

The degeneracy will depend upon the system size K and the magnitude j of the spins. We therefore use the notation

$$\bar{N}_J = \bar{N}_J(j, K) . \tag{17}$$

Similarly, each eigenvalue of J_z has some degeneracy $n_M(j, K)$.

Because every family of $(2J+1)$ states has one member $|J, M\rangle$ with each value of M such that $|M| \leqslant J$, the relationship between $\bar{N}_J$, the number of families, and n_M is

$$n_M(j, K) = \sum_{J \geqslant |M|} \bar{N}_J(j, K) . \tag{18}$$

Alternatively, we may write

$$\bar{N}_J(j, K) = n_J(j, K) - n_{J+1}(j, K) . \tag{19}$$

In order to find the degeneracies N_J of the energy eigenvalues, we first find n_M using a recursion relation, and then derive the N_J using equations (16) and (19).

The recursion relation for n_M follows from some elementary facts about the addition of angular momentum in quantum mechanics.

Suppose that two systems with angular momentum operators $\boldsymbol{J}^{(1)}$ and $\boldsymbol{J}^{(2)}$ are combined, so that the operator for total angular momentum is

$$\boldsymbol{J} = \boldsymbol{J}^{(1)} + \boldsymbol{J}^{(2)} . \tag{20}$$

The quantum number M for the z-component of the total angular momentum is the sum of the quantum numbers for the individual systems:

$$M = M^{(1)} + M^{(2)} . \tag{21}$$

Hence the degeneracy for this quantum number M is given by

$$n_M = \sum_{M_1+M_2=M} n^{(1)}_{M_1} n^{(2)}_{M_2} . \tag{22}$$

For our system of K spins, each with angular momentum j, we therefore have

$$n_M(j, K+1) = \sum_{m=-j}^{j} n_m(j, 1) n_{(M-m)}(j, K) . \tag{23}$$

This is the recursion relation which we need to derive the degeneracies. The values of $n_M(j, K)$ for $K = 1$ are simply

$$n_M(j, 1) = \begin{cases} 1 & \text{for } |M| \leqslant j \\ 0 & \text{otherwise} . \end{cases} \tag{24}$$

There is a close analogy between this problem and one from the theory of probability. Consider the distribution over the integers given by

$$p(n) = \begin{cases} 1/(2j+1) & \text{for } |n| \leqslant j \\ 0 & \text{otherwise} . \end{cases} \tag{25}$$

The distribution $P_K(x)$ of the random variable

$$x_K = \sum_{i=1}^{K} n_i \tag{26}$$

which is the sum of K independent integers taken from the distribution $p(n)$, obeys a recursion relation similar to (23):

$$P_{K+1}(x) = \sum_{m=-j}^{j} p(m) P_K(x-m) . \tag{27}$$

For large K, the central limit theorem [20] tells us that P_K is well approximated by a Gaussian:

$$P_K(x) \simeq \frac{1}{(2\pi S^2)^{1/2}} \exp\left(-\frac{x^2}{2S^2}\right) . \tag{28}$$

This approximation is discussed in the appendix, where we show that

$$S^2 = \frac{Kj(j+1)}{3} \tag{29}$$

so that

$$n_M(j, K) \simeq \frac{(2j+1)^K}{(2\pi S^2)^{1/2}} \exp\left(-\frac{x^2}{2S^2}\right) \tag{30}$$

for large j and K. In the appendix, we show that the convergence of the degeneracies to this approximation is uniform in j for large values of j and K. We can therefore use this approximation with confidence in the region where j and K are large.

The next step is to find $\bar{N}_J(j, K)$ using equation (19). We obtain

$$\bar{N}_J(j, K) \simeq \frac{(2j+1)^K}{(2\pi S^2)^{1/2}} \exp\left(-\frac{J(J+1)}{2S^2}\right)\left[\exp\left(-\frac{J}{2S^2}\right) - \exp\left(-\frac{J+1}{2S^2}\right)\right]. \tag{31}$$

Expanding the quantity in square brackets as a power series gives

$$\bar{N}_J(j, K) \simeq \frac{(2j+1)^K}{2S^3(2\pi)^{1/2}}(2J+1)\exp\left(-\frac{J(J+1)}{2S^2}\right)\left[1 + \mathrm{O}\left(\frac{J}{S^2}\right)\right]. \tag{32}$$

Since $|J| \leqslant Kj$, and S^2 is given by equation (29),

$$\frac{J}{S^2} \lesssim \frac{jK}{Kj^2} = \frac{1}{j} \tag{33}$$

so that when j is large, we can neglect the terms of order J/S^2 in (32). We thus arrive at our final expression for $\bar{N}$, valid when both j and K are large:

$$\bar{N}_J(j, K) \simeq \frac{(2j+1)^K}{2(2\pi)^{1/2}}\left(\frac{3}{Kj(j+1)}\right)^{3/2}(2J+1)\exp\left(-\frac{3J(J+1)}{2Kj(j+1)}\right). \tag{34}$$

5. The trace of the quantum evolution operator

The quantum-mechanical time-evolution operator U_t is defined as follows. If we have a time-dependent quantum state $\psi(t)$, then

$$U_t\psi(s) = \psi(s+t)\,. \tag{35}$$

That is, U_t carries states towards the future by a time t. It can be written in terms of the eigenstates $|e_n\rangle$ and eigenvalues E_n of the Hamiltonian:

$$U_t = \sum_n |e_n\rangle\langle e_n|\,\mathrm{e}^{-\mathrm{i}E_n t/\hbar}\,. \tag{36}$$

The trace $\mathcal{U}(t)$ of this operator gives a scalar, time-dependent quantity which is the simplest characterization of the quantum dynamics of a system:

$$\mathcal{U}(t) = \mathrm{Tr}\,U_t = \sum_n \mathrm{e}^{-\mathrm{i}E_n t/\hbar}\,. \tag{37}$$

The trace of the evolution operator, and its Fourier transform, the density of states, have often been used to study 'quantum chaos'. A large amount of theoretical work has been devoted to deriving semiclassical formulae, such as the Gutzwiller trace formula, for the density of states [21, 22]. Berry and Goldberg [7] have used $\mathcal{U}(t)$ as a simple characterization of the time dependence of a system, in the same way that it is used here.

For the interacting spin system which we consider here, $\mathcal{U}(t)$ can be written in terms of the energies E_J and their degeneracies $N_J = (2J+1)\bar{N}_J$:

$$\mathcal{U}(t) = \sum_{J=0}^{jK}(2J+1)\bar{N}_J(j, K)\,\mathrm{e}^{-\mathrm{i}E_J t/\hbar}\,. \tag{38}$$

From equations (11) and (34), we have

$$\mathcal{U}(t) \simeq 2C\sum_{J=0}^{jK}(2J+1)^2\,\mathrm{e}^{\mathrm{i}\pi J(J+1)z} \tag{39}$$

where C is the time-independent quantity

$$C = \frac{(2j+1)^K}{(32\pi)^{1/2}} \left(\frac{3}{Kj(j+1)} \right)^{3/2} \tag{40}$$

and z is a complex number,

$$z = \frac{1}{Kj(j+1)} \left(\tau + \frac{3\mathrm{i}}{2} \right). \tag{41}$$

To simplify our equations, we use the dimensionless time

$$\tau = \frac{\gamma \bar{h} t}{\pi} \tag{42}$$

and write U as a function of τ.

The last term in the sum in equation (39) is of order

$$(Kj)^2 \exp\left(-\frac{3(Kj)^2}{2Kj^2} \right) = (Kj)^2 \exp\left(-\frac{3K}{2} \right) \tag{43}$$

so that provided

$$j \ll \frac{1}{K} \exp\left(\frac{3K}{4} \right) \tag{44}$$

the error introduced by extending the sum to infinity is negligible. For large values of K, the last equation imposes only a mild restriction on j.

Also, since

$$\sum_{J=0}^{\infty} (2J+1)^2 \, \mathrm{e}^{\mathrm{i}\pi J(J+1)z} = \sum_{J=-\infty}^{-1} (2J+1)^2 \, \mathrm{e}^{\mathrm{i}\pi J(J+1)z} \tag{45}$$

we can write $\mathcal{U}(\tau)$ as a sum over both positive and negative J:

$$\mathcal{U}(\tau) \simeq C \sum_{J=-\infty}^{\infty} (2J+1)^2 \, \mathrm{e}^{\mathrm{i}\pi J(J+1)z} \, . \tag{46}$$

In both this section and section 6, we make use of the relationship between $\mathcal{U}(\tau)$ and the simpler sum $S(z)$, defined by

$$S(z) = \sum_{J=-\infty}^{\infty} \mathrm{e}^{\mathrm{i}\pi J(J+1)z} \, . \tag{47}$$

The trace $\mathcal{U}(\tau)$ can be written in terms of $S(z)$ and its derivative:

$$\mathcal{U}(\tau) = C \left(\frac{4}{\mathrm{i}\pi} \frac{\mathrm{d}S}{\mathrm{d}z} + S(z) \right). \tag{48}$$

Perhaps the most obvious way to approximate the sum (47) is to replace the sum by an integral. By using the Poisson summation formula [23], we can find out when this approximation is valid. The Poisson formula for the sum of a sequence $f(n)$ is

$$\sum_{n=-\infty}^{\infty} f(n) = \sum_{k=-\infty}^{\infty} \tilde{f}(2\pi k) \tag{49}$$

where $\tilde{f}(\omega)$ is the Fourier transform

$$\tilde{f}(\omega) = \int_{-\infty}^{\infty} \mathrm{d}t \, f(t) \, \mathrm{e}^{\mathrm{i}\omega t} \, . \tag{50}$$

Applying this formula to the sum $S(z)$ yields

$$S(z) = (\mathrm{i}z)^{-1/2} \sum_{k=-\infty}^{\infty} \exp\left(\frac{-\mathrm{i}\pi z}{4}(1 + 4k/z + 4k^2/z^2)\right). \tag{51}$$

The $k = 0$ term in this sum is the result of replacing the sum by an integral in the definition of $S(z)$ (equation (47)). Other terms are negligible when

$$-\mathrm{Im}\frac{1}{z} \gg 1 \tag{52}$$

where $\mathrm{Im}\, w$ denotes the imaginary part of a complex number w. This condition can be written as

$$x^2 \ll y(1 - y) \tag{53}$$

where $z = x + \mathrm{i}y$, or in terms of the quantities τ, j, K in equation (41),

$$\tau \lesssim j\sqrt{K}\,. \tag{54}$$

The resulting expression for $S(z)$ is

$$S(z) = \left(\frac{\mathrm{i}}{z}\right)^{1/2} \exp\left(-\frac{\mathrm{i}\pi z}{4}\right). \tag{55}$$

Combined with equations (41) and (48), this gives a simple expression for the trace $\mathcal{U}(\tau)$:

$$\begin{aligned}\mathcal{U}(\tau) &\simeq \frac{2C}{i\pi}\left(\frac{1}{\mathrm{i}z^3}\right)^{1/2} \mathrm{e}^{-\mathrm{i}\pi z/4} \\ &= \frac{2C}{\mathrm{i}\pi}\left(\frac{\mathrm{i}Kj(j+1)}{\tau + 3i/2}\right)^{3/2} \exp\left(-\frac{\pi}{8Kj(j+1)}[3 - 2\mathrm{i}\tau]\right).\end{aligned} \tag{56}$$

We have now derived a simple formula (56) for the trace of the quantum evolution operator, which is valid when the condition (44) holds, j and K are large, and the time τ is small enough to satisfy equation (54). However, we have no information so far on the behaviour of $\mathcal{U}(\tau)$ for large times.

An interesting feature of the formulae (54) and (56) is that the parameters j and K, which describe the size of each spin and the number of spins in the system, appear only in the combination $Kj(j + 1)$ (the right-hand side of equation (54) being an approximate form for $(Kj(j + 1))^{1/2}$ when j is large). This means that in the combined classical and thermodynamic limit, a single parameter

$$N = Kj(j + 1) \simeq Kj^2 \tag{57}$$

measures how far the collective behaviour of the system is removed from the small-scale, quantum-mechanical laws which govern it. We will see in section 6 that the parameter N appears again as a measure of the complexity of the trajectory of $\mathcal{U}(\tau)$ at long times.

It is well known that semiclassical approximations for the time evolution of quantum systems often break down at long times (for an excellent review, see Chirikov *et al* [2]), so we might expect that for large values of τ, the simple formula (56) will cease to be valid. In the next section, we explore the behaviour of $\mathcal{U}(\tau)$ at long times using a renormalization scheme. We shall find that the long-time behaviour of the trace is extremely complex, with complexity increasing as we increase the values of the parameters j and K.

6. Long-time behaviour of the model

If we fix the parameters j and K which describe the system, and allow it to evolve with time $t = \pi\tau/\gamma\bar{h}$, then the complex number

$$z = \frac{1}{Kj(j+1)}\left(\tau + \frac{3\mathrm{i}}{2}\right) \tag{58}$$

moves along a path in the complex plane which starts (at $\tau = 0$) on the imaginary axis and has a real part which is proportional to the time. Increasing the value of $Kj(j+1)$ moves this path closer to the real axis. Equation (55) gives us the behaviour of $S(z)$ for the first part of this path, where $\tau \lesssim j\sqrt{K}$. In this section, we investigate the remaining part of the path, where the approximation (55) fails.

By repeatedly applying a transformation to the simple sum $S(z)$ which was defined by equation (47), we shall examine its behaviour near the real line. Using the relationship (48) between $\mathcal{U}(\tau)$ and $S(z)$, we shall then be able to draw some conclusions about how $\mathcal{U}(\tau)$ behaves at long times for large values of j and K.

A scheme related to the one which we use here has been used by Berry and Goldberg [7] to examine the properties of a sum $S_L(\tau)$, similar to $S(z)$, which describes a single precessing quantum spin. They found that certain properties of the sum depended on whether the dimensionless time was rational or irrational.

6.1. Jacobian elliptic Theta-functions and the imaginary transformation

The transformation which we shall use is based on the properties of the Jacobian elliptic Theta-function $\Theta_3(a|b)$. The Theta-functions are discussed by Whittaker and Watson [24], whose notation we use.

The Theta-function is a complex function of two complex variables, a and b. It is defined by the equation

$$\Theta_3(a|b) = \sum_{-\infty}^{\infty} \mathrm{e}^{\mathrm{i}\pi(bn^2+2na)}\,. \tag{59}$$

From the definition of $S(z)$ (equation (47)), we can see that

$$S(z) = \Theta_3\left(\frac{\pi z}{2}\middle| z\right). \tag{60}$$

The property of $\Theta_3(a|b)$ which allows us to derive a renormalization map for $S(z)$ is known as *Jacobi's imaginary transformation* [24]. It is simply the equation

$$\Theta_3(a|b) = (-\mathrm{i}b)^{-1/2}\exp\left(\frac{a^2}{\pi\mathrm{i}b}\right)\Theta_3\left(\frac{a}{b}\middle|\frac{-1}{b}\right). \tag{61}$$

To use this property, we define a function

$$\begin{aligned} T(z) &= \Theta_3\left(\frac{\pi}{2}\middle| -z\right) \\ &= \sum_{J=-\infty}^{\infty}(-1)^J\,\mathrm{e}^{-\mathrm{i}\pi J^2 z}\,. \end{aligned} \tag{62}$$

The imaginary transformation (61) implies that $S(z)$ and $T(z)$ are related by the equations

$$S(z) = (-\mathrm{i}z)^{-1/2}\mathrm{e}^{-\mathrm{i}\pi z/4}T(1/z) \tag{63}$$

and

$$T(z) = (-\mathrm{i}z)^{-1/2}\,\mathrm{e}^{\mathrm{i}\pi/4z}S(1/z)\,. \tag{64}$$

The functions S and T share a periodicity in the real part of z, with period 1. That is, they obey the equations

$$S(z+n) = S(z) \tag{65}$$

and

$$T(z+n) = T(z) \tag{66}$$

where n is any integer. These two equations can be derived using the definitions (47) and (62), and the identity $e^{2in\pi} = 1$.

The equations (63)–(66) are the results which we shall need to construct the renormalization scheme.

6.2. The continued-fraction map

With the results of the last section in mind, we define the renormalization map

$$f(z) = \frac{1}{z} - m(z) \tag{67}$$

where $m(z)$ is an integer, chosen for each z so that $f(z)$ lies in the strip

$$\Gamma = \{z = x + iy : 0 < x \leqslant 1\} \tag{68}$$

in the complex plane. The function f then maps Γ onto itself, and can be thought of as the definition of a discrete-time dynamical system on the phase-space Γ.

This mapping is useful because, as we can see from equations (63)–(66), the function $S(z)$ is related to the function $T(z)$ by the transformation $z \to 1/z$, and both $S(z)$ and $T(z)$ are invariant under the transformation $z \to z + n$. In section 6.4, we shall see how we can use these properties to draw conclusions about $S(z)$.

We refer to f as the *continued-fraction map*, because its restriction to the real line is closely related to the continued-fraction representation of real numbers [25]. Continued fractions are important in the theory of numbers, and have applications in the theory of dynamical systems [26] and in numerical analysis [27].

Any real number x in the range $0 < x \leqslant 1$ has a unique representation as a continued fraction,

$$x = \cfrac{1}{a_1 + \cfrac{1}{a_2 + \cfrac{1}{a_3 + \cdots}}} \tag{69}$$

where each a_i is a positive integer. Following Khinchin [25], we use the notation

$$[a_1, a_2, a_3, \ldots] = \cfrac{1}{a_1 + \cfrac{1}{a_2 + \cfrac{1}{a_3 + \cdots}}}\,. \tag{70}$$

If x is rational, the fraction is finite, and the number x is exactly equal to the finite continued fraction

$$[a_1, a_2, \ldots, a_n] = \cfrac{1}{a_1 + \cfrac{1}{a_2 + \cfrac{1}{\ddots \cfrac{1}{a_n}}}}\,. \tag{71}$$

However, for an irrational number x, the continued fraction is infinite. For example,

$$\frac{1}{\sqrt{3}} = [1, 2, 1, 2, 1, 2, \ldots] . \tag{72}$$

Truncating the fraction after some a_n yields a rational approximation p_n/q_n to x, given by

$$\frac{p_n}{q_n} = [a_0, a_1, \ldots, a_n] . \tag{73}$$

This approximation is the best which can be achieved with denominator $\leqslant q_n$, and successive approximations converge to x [25]:

$$\lim_{n\to\infty} \frac{p_n}{q_n} = x . \tag{74}$$

The map f can be used to derive the continued-fraction representation for a real number x. If

$$x = [a_1, a_2, a_3, \ldots] \tag{75}$$

then

$$f(x) = [a_2, a_3, \ldots] \tag{76}$$

and

$$a_1 = m(x) . \tag{77}$$

Repeated application of the map f gives the integers a_i which determine the continued fraction:

$$a_{i+1} = m(f^i(x)) . \tag{78}$$

By repeatedly applying the continued-fraction map f, we define a discrete-time dynamical system on the interval $(0, 1]$. The invariant distribution for this map was discovered by Gauss, but a full treatment of the ergodic properties of the system was given only recently [28].

6.3. The continued-fraction map in the complex plane

In this paper we are concerned with the properties of the dynamical system defined by f, not on the real line, but in the complex plane. We shall see that as long as we avoid the real line, the behaviour of f is quite simple, and more easily described than the behaviour on the real line.

We use the symbol Γ' to denote the set Γ with the real line removed. As we saw in the previous section, the function f maps the region Γ, defined by equation (68), onto itself. Clearly, if z is on the real line, so is $f(z)$ and also all the pre-images w such that $f(w) = z$. Hence we can also regard f as a map from Γ' onto itself.

We partition Γ' into a countable set of regions $\{\Gamma_n : n = 0, 1, \ldots\}$, defined in terms of the map f as follows.

A complex number z is in Γ_0 if it is a period-two fixed point of the map f; that is, if $f^2(z) = z$, or

$$\left(\frac{1}{z} - m_1\right)^{-1} - m_2 = z \tag{79}$$

for some pair of non-negative integers m_1, m_2. This equation can be rearranged to give a quadratic in z which has real roots unless $m_1 = m_2 = 0$. So if z is a period-two fixed-point in Γ', we must have $m(z) = 0$, and hence

$$\mathrm{Re}\frac{1}{z} \leqslant 1 \tag{80}$$

where $\mathrm{Re}\, w$ denotes the real part of a complex number w. If we write z in terms of its real and imaginary parts,

$$z = x + \mathrm{i}y \tag{81}$$

then the condition for z to be in Γ_0 is

$$y^2 \geqslant x(1-x)\,. \tag{82}$$

The set Γ_0 therefore covers the whole of Γ apart from the interior of the circle of radius $\frac{1}{2}$ with centre $z = \frac{1}{2}$ (figure 1).

We now define Γ_n, for $n > 0$, to be the set of points z which take exactly n iterations of the map f to reach Γ_0. That is,

$$\Gamma_n = \left\{z : f^n(z) \in \Gamma_0 \text{ but } f^{n-1}(z) \notin \Gamma_0\right\}. \tag{83}$$

For $n > 1$, we have

$$\Gamma_n = f^{-1}(\Gamma_{n-1}) \tag{84}$$

where $f^{-1}(A)$ denotes the pre-image of the set A.

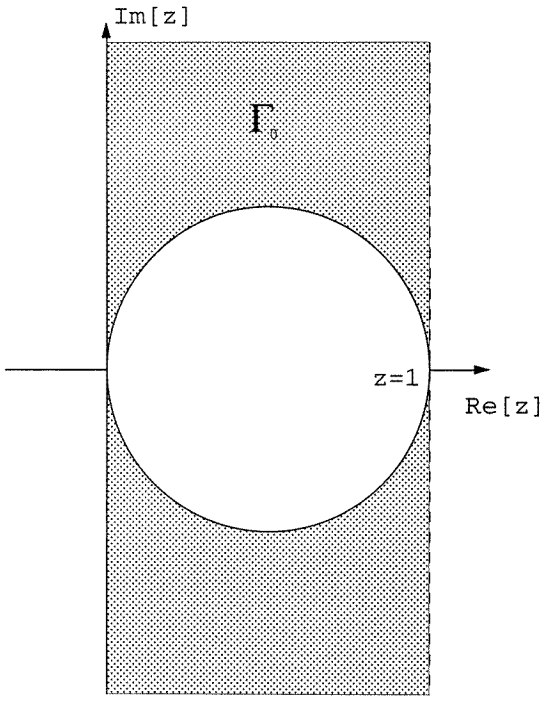

Figure 1. The regions Γ and Γ_0 in the complex plane. Γ is the whole strip $0 < \mathrm{Re}\, z \leqslant 1$, including the circle and the shaded region in the diagram. Γ_0 is the shaded region only.

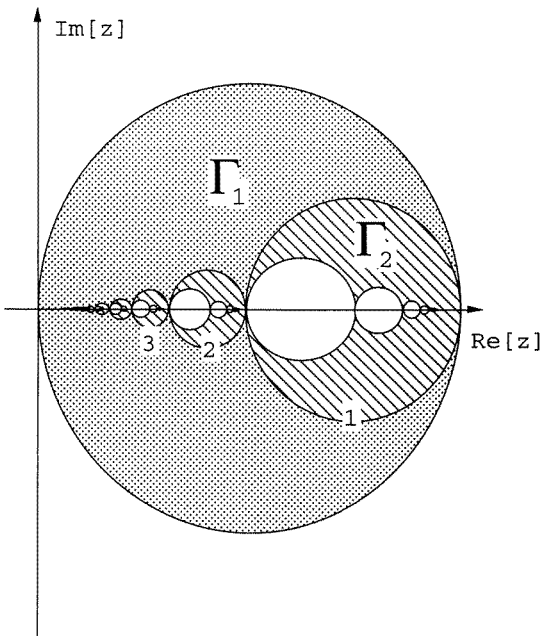

Figure 2. The regions Γ_1 and Γ_2 in the complex plane. Subsets of Γ_2 are numbered $1, 2, \ldots$.

Figure 2 is a picture of the sets Γ_1 and Γ_2. The curve which separates Γ_1 from Γ_2 consists of all the pre-images of the circle in figure 1 under the map f. As we can see from figure 2, the set Γ_2 consists of an infinite sequence of disjoint regions, each corresponding to a different value of $m(z)$ in equation (67). We number these $1, 2, 3, \ldots$ as in the diagram. Region m is mapped into the circle in figure 1 by the function $z \to 1/z - m$.

Each of the disjoint regions in figure 2 contains an image of the entire sequence of regions within itself. These sub-regions contain the set Γ_3. The boundaries of the sets $\Gamma_1, \Gamma_2, \ldots$ form a self-similar pattern in the complex plane, which has detail on increasingly fine scales as we approache the real axis (figure 3). As we shall see, this detail is related to small-scale structure in the function $S(z)$.

The union of all the regions $\Gamma_0, \Gamma_1, \ldots$ is the set Γ'. This means that any complex number z which has $\mathrm{Re}\, z \neq 0$ will reach Γ_0 after a finite number of applications of the map f.

This analysis of the map f allows us to define a unique continued-fraction representation for complex numbers in Γ'. If z is in Γ_n, then $f^n(z)$ is in Γ_0, so we can write

$$\tilde{z} = f^n(z) \tag{85}$$

where $\tilde{z}$ is in Γ_0. Using the definition of f (equation (67)), we can invert this equation, finding

$$z = \cfrac{1}{a_1 + \cfrac{1}{a_2 + \cfrac{1}{\ddots \cfrac{1}{a_n + \tilde{z}}}}} \tag{86}$$

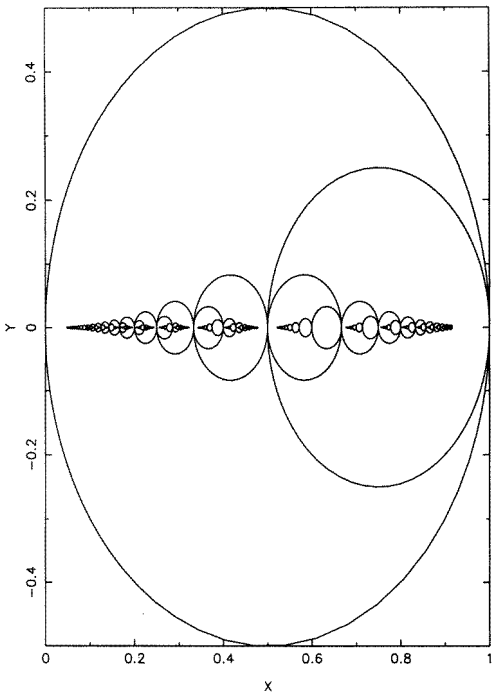

Figure 3. The boundaries of the regions Γ_i in the complex plane.

or, in the notation of equation (71),

$$z = [a_1, a_2, a_3, \ldots, a_n, 1/\tilde{z}]\,. \tag{87}$$

With the convention that n is chosen, as above, to be the smallest integer such that $f^n(z) \in \Gamma_0$, this equation defines a unique continued-fraction representation for any complex number z in Γ'.

We can think of the integers $\{a_1, a_2, \ldots, a_n\}$ as the address of the point z in the complex plane. z lies inside the region numbered a_1 in figure 2. Inside this region is an infinite sequence of subregions, and z lies inside the a_2th of these. We continue, specifying smaller regions of the complex plane, until we reach the last non-zero a_j. This specifies which of an infinite sequence of pre-images of Γ_0, all contained within the region defined by $a_1, a_2, \ldots, a_{j-1}$, contains z. Figure 4 shows a set of these pre-images. The location of z within one of these pre-images is specified by $\tilde{z}$.

As the time τ increases, and z follows its simple straight-line trajectory through the complex plane according to equation (41), the complex number $\tilde{z}$ follows a much more complicated path. When τ is small, z is in Γ_0 and so $\tilde{z} = z$. However, when z reaches the boundary of Γ_0 and crosses into Γ_1, the two complex numbers part and $\tilde{z}$ begins crossing and re-crossing the set Γ_0. As z moves into the parts of the complex plane which have finely detailed structure in figure 3, $\tilde{z}$ must cross Γ_0 more and more frequently.

6.4. Implications for the function S(z)

We shall now use the knowledge which we have collected about the dynamics of the map f to examine the complex function $S(z)$ defined by equation (47). Equations (63)–(66), which

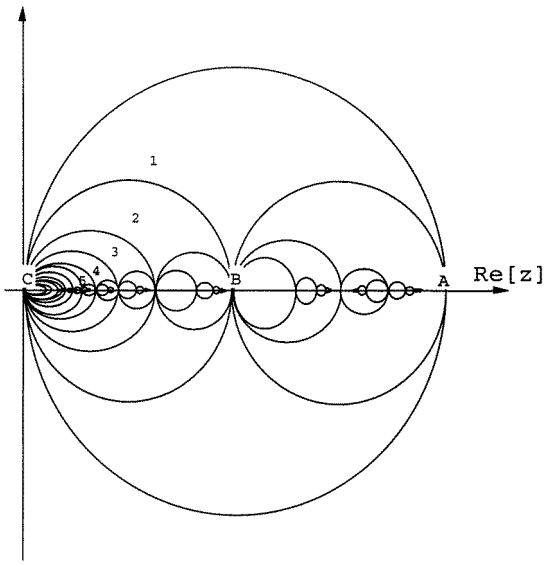

Figure 4. An infinite set of pre-images of Γ_0 (regions numbered 1, 2, 3, ...). In region 1, $S(z)$ has square-root singularities at the points A and B, and an essential singularity at C.

describe the properties of $S(z)$ and the related function $T(z)$ under some transformations in the complex plane, will lead us to an equation which shows how the function $S(z)$ changes when z is repeatedly transformed by the map f. We use the notation

$$z_k = f^k(z) \tag{88}$$

to simplify our equations.

The function $T(z)$ transforms in a particularly simple way under an even number of repeated applications of the map f. From equations (63)–(66), we obtain

$$T(z) = (zz_1)^{-1/2} \exp\left(\frac{\mathrm{i}\pi}{4}\left[\frac{1}{z} - z_1\right]\right) T(z_2)\,. \tag{89}$$

Since z and z_1 are related by the map f, we have simply

$$T(z) = \left(\frac{i^{m(z)}}{zz_1}\right)^{1/2} T(z_2). \tag{90}$$

If we apply the transformation repeatedly, we obtain, for even n,

$$T(z) = i^{[m(z)+m(z_2)+\cdots+m(z_{n-2})]/2}(zz_1z_2\cdots z_{n-1})^{-1/2}T(z_n). \tag{91}$$

By combining equations (63) and (64) with the last equation, we find a similar expression for $S(z)$, also valid when n is even:

$$S(z) = \mathrm{i}^{[m(z_1)+m(z_3)+\cdots+m(z_{n-3})]/2} \exp\left(\frac{\mathrm{i}\pi}{4}\left[\frac{1}{z_{n-1}} - z\right]\right) S(z_n)\,. \tag{92}$$

To put this equation in its final form, we take the complex modulus, and neglect the appearance of z in the exponent, since we shall be interested in the limiting behaviour as the imaginary part of z becomes small. We then write z_{n-1} in terms of z_n, obtaining

$$|S(z)| \simeq \frac{1}{|zz_1\cdots z_{n-1}|^{1/2}} |\mathrm{e}^{-\mathrm{i}\pi z_n/4} S(z_n)|\,. \tag{93}$$

For values of z in one of the sets Γ_m where m is even, we can use this equation as it stands, since in this case $\tilde{z} = z_n$. We re-write (93) as

$$|S(z)| \simeq \frac{1}{|zz_1 \cdots z_{n-1}|^{1/2}} R(\tilde{z}) \tag{94}$$

where

$$R(\tilde{z}) = |\mathrm{e}^{-\mathrm{i}\pi\tilde{z}/4} S(\tilde{z})| = \mathrm{e}^{\pi\tilde{y}/4} |S(\tilde{x} + \mathrm{i}\tilde{y})| \tag{95}$$

and $\tilde{z} = \tilde{x} + \mathrm{i}\tilde{y}$. We note that in this case $\tilde{z}$ lies in the upper half of the region Γ_0; that is, $\tilde{y} > 0$.

When z lies in a set Γ_m for which m is odd, we set $n = m + 1$, so that

$$z_n = f(\tilde{z}) = \frac{1}{\tilde{z}} \tag{96}$$

and

$$|S(z)| \simeq \frac{1}{|zz_1 \cdots z_{n-1} z_n|^{1/2}} R\left(\frac{1}{\tilde{z}}\right) \tag{97}$$

where now $1/\tilde{z}$ lies in the upper half of Γ_0.

Equations (94) and (97) give us the modulus of the function $S(z)$, for any z in Γ', in terms of the function $R(z)$ evaluated at points in the upper half of Γ_0. Before we can draw conclusions about the behaviour of $S(z)$, we must first look at $R(z)$.

In section 5, we derived equation (55), which is an approximate expression for $S(z)$, valid when $y(1-y) \gg x^2$. This gives us the approximate behaviour of $R(z)$ in the corner of Γ_0 near $z = 0$: in this region

$$R(z) \simeq \frac{1}{|z|^{1/2}} \,. \tag{98}$$

The approximation (55) is also valid when $x < 0$. Since, from equation (65), $S(z+1) = S(z)$, the behaviour of $R(z)$ close to $z = 1$ is similar to that near $z = 0$. In the corner of Γ_0 close to $z = 1$, we therefore have

$$R(z) \simeq \frac{1}{|z-1|^{1/2}} \,. \tag{99}$$

It is clear from the definition of $S(z)$ (equation (47)) that, for large values of y, all terms in the sum apart from those with $J(J+1) = 0$ are exponentially small. For large values of y, we therefore have $S(z) \simeq 2$, and

$$R(z) \simeq 2\mathrm{e}^{\pi y/2} \,. \tag{100}$$

Figure 5 is a plot of the function $R(z)$. We can see that the three equations (98)–(100) capture, at least qualitatively, the behaviour of the function in the part of Γ_0 above the real axis. Away from the two singularities at $z = 0$ and $z = 1$, $R(z)$ varies smoothly, being well approximated by equation (100). The only significant features of $R(z)$ in the region of interest are the three singularities described by equations (98)–(100): square-root singularities at $z = 0$ and at $z = 1$, and an essential singularity at infinity.

We are now ready to draw some conclusions about the behaviour of the function $S(z)$ near the real line. If the set Γ_m containing z has an even value of m, then we can use equation (94). As we allow z to vary within the set Γ_m, most of the variation in $S(z)$ will come from changes in $\tilde{z}$. Therefore within each pre-image of Γ_0 in figure 4, there are three singularities of $S(z)$: one for each of the three singularities in $R(z)$. For example, in region 1, there are square-root singularities at the points A and B, and an essential singularity at the point C.

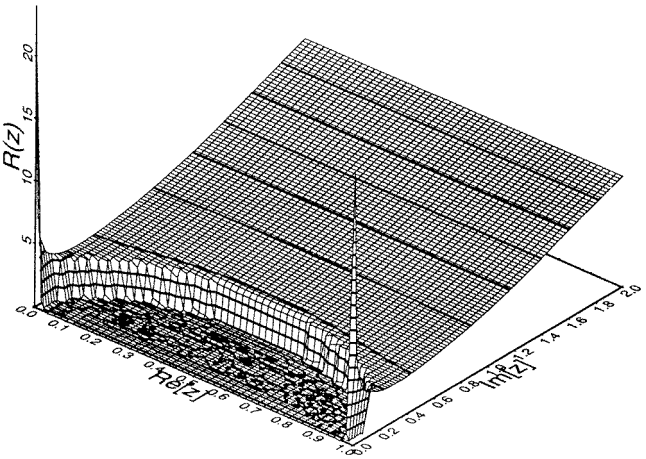

Figure 5. The function $R(z)$, evaluated in the part of Γ_0 above the real axis. The form of the function is dominated by the three singularities at $z = 0$, $z = 1$ and $z = \infty$.

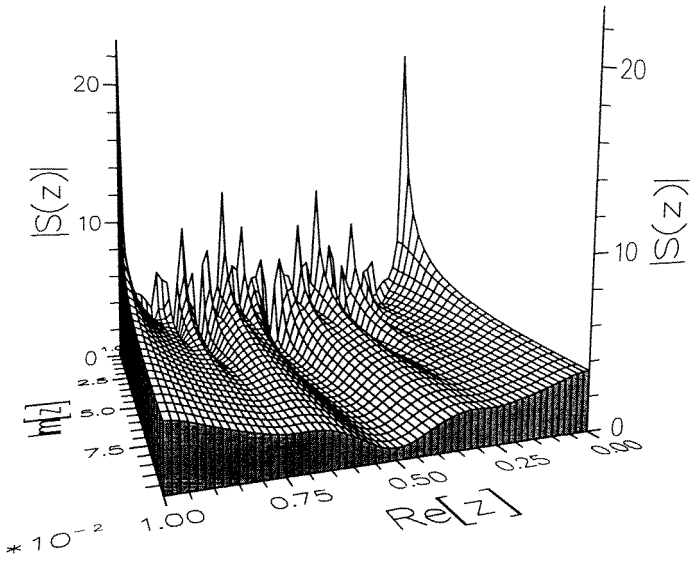

Figure 6. The modulus of the function $S(z)$.

When m is odd, we must use equation (97). The situation is very similar. The only difference is that we must use $R(1/z)$ instead of $R(z)$. Hence in this case we have square-root singularities at the points B and C, and an essential singularity at A.

We now have a picture of the function $S(z)$ throughout the upper half of Γ'. In the region

$$x^2 \ll y(1-y) \tag{101}$$

$S(z)$ varies smoothly according to equation (55), with the square-root singularity at $z = 0$ dominating the function. As we increase the x-coordinate, we move away from this region where $S(z)$ is simple and smooth, into areas of fine detail. Inside each pre-image of Γ_0,

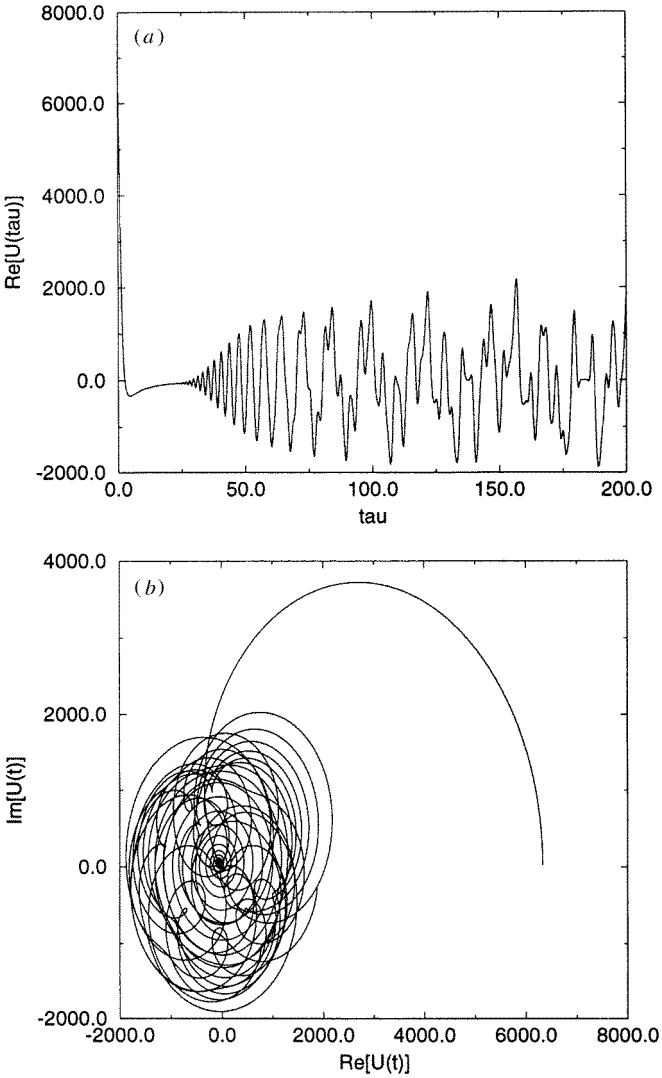

Figure 7. $\mathcal{U}(\tau)$ as a function of τ: (*a*) shows the real part of $\mathcal{U}(\tau)$ as a function of τ for $j = 10$, $K = 10$; (*b*) shows the trajectory of $\mathcal{U}(\tau)$ in the complex plane for the same values of j and K; (*c*) and (*d*) show the same information for the values $j = 50$, $K = 100$.

there are three singularities which influence the behaviour of $S(z)$, and it is only when we near these singularities that the function varies rapidly. All the singularities are on the real line, and as we move closer to the real line, the pattern formed by the sets Γ_i becomes more complex, and the behaviour of $S(z)$ becomes more complex. Figure 6 is a plot of the modulus of $S(z)$, which illustrates some of this complexity.

6.5. The trace of the quantum evolution operator at long times

Now that we have a qualitative picture of the behaviour of $S(z)$, we can see how the trace of the quantum evolution operator, $\mathcal{U}(\tau)$, changes with increasing dimensionless time τ.

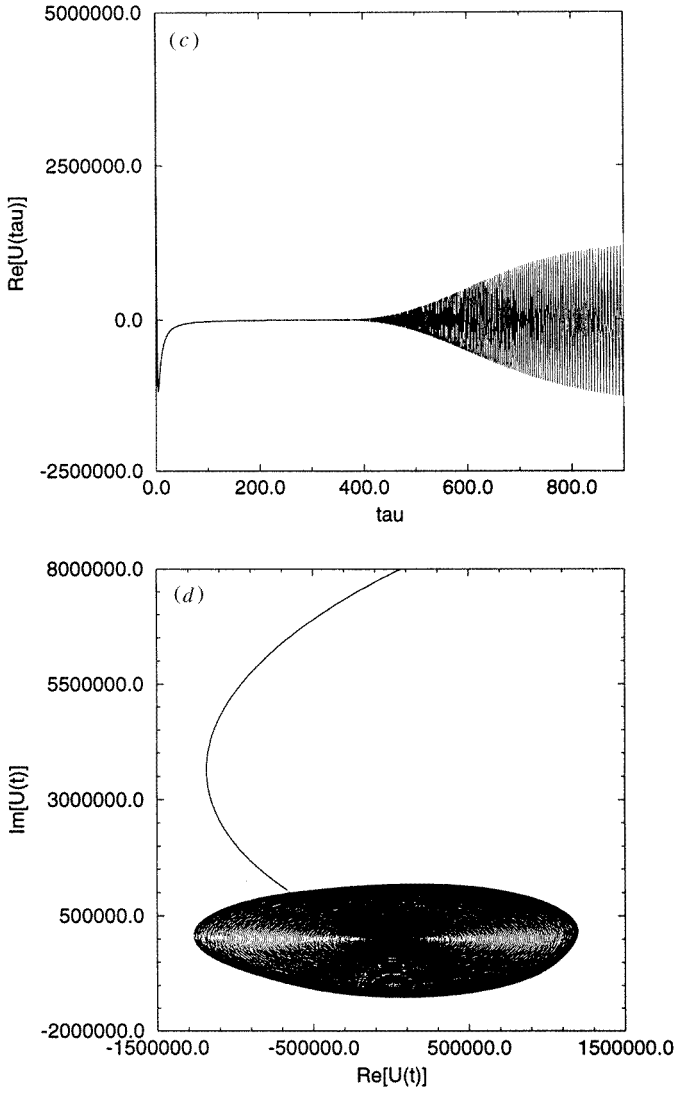

Figure 7. Continued.

The trace is related to the derivative of $S(z)$ by equation (48). As we saw in section 5, at times less than a critical time $\tau_c \sim j\sqrt{K}$, or in terms of the real time t,

$$t_c \sim \frac{j\sqrt{K}}{\gamma\bar{h}} \tag{102}$$

an approximation gives a simple expression (56) for $\mathcal{U}(\tau)$. As $S(z)$ varies in a more complicated way for larger values of x, the behaviour of $\mathcal{U}(\tau)$ for large values of τ is similarly complicated. As we can see from equation (41), the imaginary part of z is inversely proportional to $j(j+1)K$, where K is the number of spins and j is the angular momentum of each spin. Therefore increasing the value of j or of K moves the trajectory of z (equation (41)) closer to the real axis, leading to more complex behaviour of $S(z)$ and also of $\mathcal{U}(\tau)$.

Figure 7 shows how the trace of U_t varies with τ for two different values of j and K. These plots were obtained by summing the series (39) directly. We can clearly see the part of the trajectory where $\tau \ll j\sqrt{K}$ and the time dependence is simple. For large values of τ, $\mathcal{U}(t)$ follows a more complicated path in the complex plane. For values of τ of order $j\sqrt{K}$, we have regular oscillations which stem from the $k = \pm 1$ terms in equation (51).

The function $\mathcal{U}(\tau)$, the trace of the quantum-mechanical evolution operator, does not give us a complete picture of the time dependence of a quantum system. However, since it is the sum of the time dependences of all the eigenstates, it does give an indication of the way typical quantum-mechanical quantities evolve with time.

7. Conclusion

For the model system which we have studied, there are two very different regimes of time dependence for the trace of the evolution operator. For 'short' times, the time dependence is simple, but for longer times it is much more complicated.

This breakdown of a simple approximation at long times is behaviour which we expect from a semiclassical limit. What is more interesting is the way in which this situation changes when we vary j, the size of each spin, and K, the number of spins. The time at which the simple approximation breaks down (equation (102)) grows with K and j, depending on the parameter $N = Kj^2$. The parameter N also appears in the approximation (56) for $\mathcal{U}(\tau)$ at short times, and as a measure of the complexity of a trajectory of $\mathcal{U}(\tau)$ at long times. So N is a single parameter which controls the combined thermodynamic–classical limit.

As we saw in section 1, we expect chaos to shorten the time of validity of the semiclassical approximation so that the time when the approximation breaks down is proportional to the logarithm of $1/\overline{h}$. The algebraic dependence of the critical time (equation (102) on $\overline{h}$ and on j and K is therefore a sign that the underlying classical dynamics of our system is not strongly chaotic. This is not a surprise, given the simple Hamiltonian (10).

The results of this paper are a reminder that the semiclassical limit of quantum mechanics, although it provides a simplifying approximation for some calculations, is not uniformly simple or easy to characterize. At long times the semiclassical limit is irregular and complex. The question which motivated the research presented here was the following: does increasing the size of a system diminish this complexity, leading to a simple and well behaved combined thermodynamic–classical limit? If this were so, it would suggest that the difficulties associated with the classical limit in small systems are not as important as they seem: they are smoothed out when we move to a macroscopic scale. But, at least in the case of the spin system studied here, the limit of large system size does not make the situation more straightforward. Rather, increasing the size of the system reinforces the effect of the semiclassical limit, generating simplicity at short times but adding to the long-time complexity. Further work is needed to determine whether this is true more generally.

Acknowledgments

I would like to thank Peter Coveney for many stimulating discussions, and also Professor M V Berry for some helpful comments. This work was financially supported by the EPSRC.

Appendix. Convergence of degeneracies to a Gaussian

This appendix addresses the question of the convergence of the degeneracies in the spin model to a Gaussian approximation for large values of j and K.

Given the distribution

$$n_1^j(m) = \begin{cases} 1 & |m| \leqslant j \\ 0 & |m| > j \end{cases} \tag{A1}$$

we discuss the behaviour for large j, K of the multiple convolution $n_K^j(m)$, defined recursively by

$$n_{K+1}^j(m) = \sum_{m_1=-j}^{j} n_1^j(m_1) n_K^j(m - m_1)\,. \tag{A2}$$

It is a consequence of the central limit theorem (Feller 1968) that for large K, n_K^j converges to a Gaussian:

$$n_K^j(m) \to (2j+1)^K \frac{1}{(2\pi S^2)^{1/2}}\, \mathrm{e}^{-m^2/2S^2} \tag{A3}$$

where the factor $(2j+1)^K$ derives from the fact that the distribution (A1) is not normalized, and where S^2 is the variance of the multiple convolution, given by

$$S^2 = K\sigma^2 \tag{A4}$$

σ^2 being the variance of the distribution $n_1^j(m)$. The quantity σ^2 is easily calculated from the formula for the sum of the squares of the first j integers (see, for example, Arfken 1985, p 336). We thus obtain

$$S^2 = \frac{Kj(j+1)}{3}\,. \tag{A5}$$

The convergence of the multiple convolution to a Gaussian is not in doubt, since the distribution n_1^j has finite moments and satisfies the conditions for the central limit theorem. However, we shall use the Gaussian as an approximation in the region of large j and K, and so some idea of how the convergence depends on j is necessary.

We define a discrete Fourier transform

$$\tilde{f}(x) = \sum_{-\infty}^{\infty} f(m)\, \mathrm{e}^{\mathrm{i}mx} \tag{A6}$$

with the inverse

$$f(m) = \frac{1}{2\pi} \int_{-\pi}^{\pi} \mathrm{d}x\; \tilde{f}(x)\, \mathrm{e}^{-\mathrm{i}mx}\,. \tag{A7}$$

A convolution theorem holds, and so, since

$$\tilde{n}_1^j(x) = \frac{\sin(j+\frac{1}{2})x}{\sin x/2} \tag{A8}$$

we have the following expression for the multiple convolution $n_K^j(m)$:

$$n_K^j(m) = \frac{1}{2\pi} \int_{-\pi}^{\pi} \mathrm{d}x\, \mathrm{e}^{-\mathrm{i}mx} \left[\frac{\sin(j+\frac{1}{2})x}{\sin x/2} \right]^K\,. \tag{A9}$$

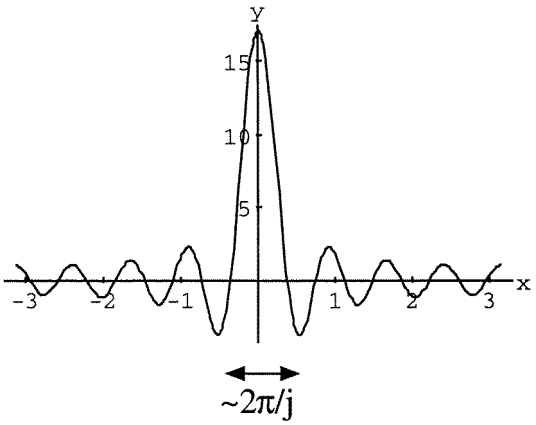

Figure A1. The function $y = \frac{\sin(j+\frac{1}{2})x}{\sin x/2}$. For large values of j, the central peak, with width of order $2\pi/j$, dominates the integral. The graph plotted here is for the value $j = 8$.

From a sketch of the function in square brackets in the last equation (figure 8), we can see that for large j, the dominant contribution to the integral comes from the small region of width $2\pi/j$ around $x = 0$.

For comparison, consider the continuous version of the discrete problem above. We take the multiple continuous convolution v_K^j of the function n_j^K defined by equation (A1). That is,

$$v_{K+1}^j(m) = \frac{1}{2\pi}\int_{-\infty}^{\infty} \mathrm{d}x\, n_1^j(x) n_K^j(m-x)\,. \tag{A10}$$

Using continuous Fourier transforms and the convolution theorem, we can easily derive a continuous version of equation (A9):

$$v_K^j(m) = \frac{1}{2\pi}\int_{-\infty}^{\infty} \mathrm{d}x\, \mathrm{e}^{-\mathrm{i}mx}\left[\frac{\sin jx}{x/2}\right]^K\,. \tag{A11}$$

Again, for large j the dominant contribution to the integral comes from a small region of width $2\pi/j$ around $x = 0$.

For the continuous version of the problem, a change in j amounts to a change of scale in m. Hence the convergence of the continuous multiple convolution to a Gaussian must be uniform in j, in the sense that the fractional error in the Gaussian approximation is independent of j.

We now compare the Fourier integrals for the discrete and continuous versions of the problem, equations (A9) and (A11). For large j, we can replace $j + \frac{1}{2}$ with j, and, in the small interval which dominates the integrals, $\sin x/2$ by $x/2$. Hence the difference between the two equations becomes small for large j. This allows us to extend the conclusion of the previous paragraph to the discrete version of the problem. That is, the convergence of the discrete multiple convolution to a Gaussian is uniform in j.

References

[1] Berry M V 1991 Asymptotics, singularities and the reduction of theories *Proc. 9th Int. Congress of Logic, Methodology and Philosophy of Science (Uppsala)* ed D Prawitz, B Skyms and D Westerstâhl (Amsterdam: North-Holland)

[2] Chirikov B V, Izrailev F M and Shepelyansky D L 1982 Dynamical stochasticity in classical and quantum mechanics *Sov. Sci. Rev.* C **2** 209–67
[3] Berman G P and Zaslavsky G M 1995 Logarithm breaking time of quantum chaos *Quantum Chaos: Between Order and Disorder* ed G Casati and B Chirikov (Cambridge: Cambridge University Press) pp 343–83
[4] Mazur P and Montroll E 1960 Poincaré cycles, ergodicity, and irreversibility in assemblies of coupled harmonic oscillators *J. Math. Phys.* **1** 70–84
[5] Lanford O E 1975 *Time Evolution of Large Classical Systems* (Berlin: Springer)
[6] Spohn H 1991 *Large Scale Synamics of Interacting Particles* (Berlin: Springer); 1980 Kinetic equations from Hamiltonian dynamics: Markovian limits *Rev. Mod. Phys.* **52** 569–616
[7] Berry M V and Goldberg J 1988 Renormalization of curlicues *Nonlinearity* **1** 1–26
Berry M V 1986 Random renormalization in the semiclassical long-time evolution of a precessing spin *Physica* **33D** 26–33
[8] Müller G 1986 Nature of quantum chaos in spin systems *Phys. Rev.* A **34** 3345–55
[9] Fisher M E 1964 Magnetism in one-dimensional systems—the Heisenberg model for infinite spin *Am. J. Phys.* **32** 343–6
[10] Millard K and Leff H S 1971 Infinite-spin limit of the quantum Heisenberg model *J. Math. Phys.* **12** 1000–5
[11] Nakamura K 1993 *Quantum Chaos: a New Paradigm for Nonlinear Dynamics* (Cambridge: Cambridge University Press)
[12] Pellegrino G Q, Furuya K and Nemes M C 1993 Quantal and classical manifestations of symmetry breaking in the integrable two-spin system *Chaos, Solitons Fractals* **3** 327–41
[13] Gaspard P and van Ede van der Pals P 1995 Level curvatures and many-spin quantum systems *Chaos, Solitons Fractals* **5** 1183–99
[14] Bethe H 1931 *Z. Phys.* **71** 205–26 (Engl. transl. 1993 On the theory of metals, 1: eigenvalues and eigenfunctions of a linear chain of atoms ed D C Mattis *The Many-body Problem: an Encyclopedia of Exactly Solved Models in One Dimension* (Singapore: World Scientific) pp 689–716)
[15] Lieb E, Schultz T and Mattis D 1961 Two soluble models of an antiferromagnetic chain *Ann. Phys.* **16** 407–66; Also reprinted 1993 *The Many-body Problem: an Encyclopedia of Exactly Solved Models in One Dimension* ed D C Mattis (Singapore: World Scientific)
[16] Mattis D C (ed) 1993 *The Many-body Problem: An Encyclopedia of Exactly Solved Models in One Dimension* (Singapore: World Scientific)
[17] Tóth B 1990 Phase transition in an interacting Bose system—an application of the theory of Ventsel and Friedlin *J. Stat. Phys.* **61** 749–64
[18] Penrose O 1991 Bose–Einstein condensation in an exactly soluble system of interacting particles *J. Stat. Phys.* **63** 761–81
[19] Messiah A 1969 *Quantum Mechanics* vol II (Amsterdam: North-Holland)
[20] Feller W 1968 *An Introduction to Probability Theory and its Applications* vol I (New York: Academic/Wiley)
[21] Gutzwiller M C 1990 *Chaos in Classical and Quantum Mechanics* (New York: Springer)
[22] Littlejohn R G 1995 Semiclassical structure of trace formulas *Quantum Chaos: Between Order and Disorder*, eds G Casati and B Chirikov (Cambridge: Cambridge University Press) pp 343–404
[23] Morse P H and Feshbach H 1953 *Methods of Theoretical Physics* (New York: McGraw-Hill) p 467
[24] Whittaker E T and Watson G N 1902 *A Course of Modern Analysis* (Cambridge: Cambridge University Press) ch XXI
[25] Khinchin A Ya 1964 *Continued Fractions* (Chicago, IL: University of Chicago Press)
[26] The most famous application is in the KAM theorem of Kolmogorov, Arnold and Moser. For an introduction, see Tabor M 1989 *Chaos and Integrability in Nonlinear Dynamics* (New York: Wiley) ch 3.4
[27] Knuth D E 1981 *The Art of Computer Programming vol 2: Seminumerical Algorithms* 2nd edn (New York: Addison-Wesley)
[28] See Mayer D and Roepstorff G 1987 On the relaxation time of Gauss's continued-fraction map: I: the Hilbert-space approach *J. Stat. Phys.* **47** 149–71; 1988 On the relaxation time of Gauss's continued-fraction map: II: the Banach-space approach *J. Stat. Phys.* **50** 331–44 and references therein